ARTICLE

$Fe_{48}Co_{52}$ Alloy Nanowire Arrays: Effects of Magnetic Field Annealing

Hai-lin Su[a,b*], Shao-long Tang[b*], Rui-long Wang[b], Yi-qing Chen[a], Chong Jia[a], You-wei Du[b]

a. School of Materials Science and Engineering, Hefei University of Technology, Hefei 230009, China
b. National Laboratory of Solid State Microstructure and Department of Physics, Nanjing University, Nanjing 210093, China

(Dated: Received on May 16, 2008; Accepted on November 16, 2008)

The effects of magnetic field annealing on the properties of $Fe_{48}Co_{52}$ alloy nanowire arrays with various interwire distances (D_i=30-60 nm) and wire diameters (D_w=22-46 nm) were investigated in detail. It was found that the array's best annealing temperature and crystalline structure did not show any apparent dependence on the treatment of applying a 3 kOe magnetic field along the wire during the annealing process. For arrays with small D_w or with large D_i, the treatment of magnetic field annealing also had no obvious influence on their magnetic performances. However, such a magnetic field annealing constrained the shift of the easy magnetization direction and improved the coercivity and the squareness obviously for arrays with large D_w or with small D_i. The difference in the intensity of the effective anisotropic field within the arrays was believed to be responsible for this different variation of the array's magnetic properties after magnetic field annealing.

Key words: FeCo alloy, Nanowire array, Magnetic field annealing, Magnetic property, Effective anisotropic field

I. INTRODUCTION

Artificial magnetic nanowire arrays have attracted much attention in recent years due to their potential application for high density recording media and multifunctional sensors [1-3]. Template methods, which have low cost and high yield, are usually adopted to synthesize these nanowire arrays. Electrodeposition of highly ordered uniform nanoarrays into an anodic aluminum oxide (AAO) template is one of the most popular methods due to its simple operation and inexpensive apparatus. Generally, it consists of two types: the alternating current (AC) electrodeposition and the direct current (DC) electrodeposition. The former one is simpler and amenable to industrial scale processing because it requires fewer processing steps, such as removing the aluminum substrate and the alumina barrier layer [4]. It has been used to fabricate many magnetic nanowire arrays, including Fe, Co, Ni, NiPb, FeNi, CoPt, FePb, FeCo, and FeCoNi, etc. [5-14]. Among these nanowire arrays, the FeCo array has attracted much attention in the past five years due to the following properties of FeCo alloy: good antioxidant ability, low-temperature coefficients of coercivity and remanence, high Curie temperature, and the highest saturation magnetization in transition metals and alloys [15-27]. In our previous work, we studied the influences of the magnetostatic interaction between nanowires and the annealing treatment on the final magnetic performance of the FeCo alloy nanowire array in detail [21,23,24]. It was found that annealing in hydrogen atmosphere can improve the magnetic properties of the arrays with weak magnetostatic interaction obviously and the best annealing temperature for FeCo alloy nanowire array is 550 °C. Through regulating the wire diameter D_w and the interwire distance D_i, the highest reported coercivity H_c and squareness M_r/M_s for nanowire arrays were finally obtained in the annealed $Fe_{48}Co_{52}$ array with D_w of about 22 nm and D_i of about 50 nm [23].

It is well known that the magnetic field is a powerful physical factor which has great influence on materials' properties. Its application to improve the microstructure and the performance of the material has become more and more popular in recent years [28,29]. But to the best of our knowledge, no report about FeCo alloy nanowire array annealed in a magnetic field has been published yet. In this work, we selected the $Fe_{48}Co_{52}$ alloy nanowire arrays fabricated by AC electrodeposition as the objects of study. A magnetic field of 3 kOe was applied along the wire during the annealing process. The influences of the magnetic field annealing on the crystalline structure and the magnetic properties of the $Fe_{48}Co_{52}$ alloy nanowire array were studied in detail.

*Author to whom correspondence should be addressed. E-mail: suhlnju@yahoo.com.cn, tangsl@nju.edu.cn, Tel.: +86-13515514127

 ©2009 Chinese Physical Society

II. EXPERIMENTS

A. Preparation of AAO templates

Highly ordered AAO templates were prepared, as described previously, by anodic oxidation of 99.999% pure aluminum foils in sulfuric acid solution via a two-step anodizing process [30,31]. Before the anodization, the aluminum foils were firstly degreased in acetone and annealed at 500 °C in hydrogen atmosphere for 2 h. Then, the annealed aluminum foils were polished in a mixed solution of ethanol and choric acid ($HClO_4$) under a constant current of 1 A for 2 min. As the first step of the anodization, the polished aluminum foils were anodized at different voltages (10-25 V) in 0.3 mol/L H_2SO_4 at 0 °C for 10 h to get different interpore distances (30-60 nm). The formed alumina was then removed by a mixture of 0.4 mol/L H_3PO_4 and 0.2 mol/L H_2CrO_4 at 60 °C for 10 h, and the aluminum sheet was reanodized under the same conditions as the first step for 4 h. To get different pore diameters (22-46 nm), the templates were etched in 0.3 mol/L H_3PO_4 at 30 °C for various time (0-20 min).

B. Preparation of annealed FeCo alloy nanowire arrays

Nanowire arrays with various D_i (30, 40, 50, 60 nm) and D_w (22, 26, 32, 40, 46 nm) were prepared by AC electrodepositing FeCo alloy into the formed AAO templates. The electrodeposition was carried out in an electrolyte consisting of 0.095 mol/L $FeSO_4{\cdot}7H_2O$, 0.125 mol/L $CoSO_4{\cdot}7H_2O$, 0.6 mol/L boric acid, and 1 g/L ascorbic acid at a pH value of about 4.0. The voltage and the frequency used in electrodeposition were 16 V and 50 Hz, respectively. Lengths L of nanowires within different templates were kept the same as about 2 μm by controlling the deposition time.

All the as-deposited samples, comprising the FeCo alloy nanowires and the AAO templates, were cut into two equal parts and divided into two groups, Group M and Group H. Both groups were then annealed at temperatures ranging from 390 °C to 590 °C in hydrogen atmosphere for 30 min. During the annealing process, a magnetic field of 3 kOe was applied in the direction parallel to the wire axis for the arrays of Group M, while the arrays of Group H were annealed without applying any magnetic field.

C. Characterization

X-ray diffraction (XRD, D/Max-RA with Cu Kα radiation) and an induction-coupled plasma spectrometer (ICP, Jarell-Ash, J-A1100) were used to investigate the crystalline structure and the composition of nanowire arrays, respectively. Magnetic properties were measured by a vibrating sample magnetometer (VSM, Lakeshore, Model 7300 series) at the room temperature.

III. RESULTS AND DISCUSSION

As reported previously, highly ordered FeCo alloy nanowire arrays with various D_i and D_w can be prepared by the above-mentioned method [23,24]. For all the annealed arrays, the atomic ratio of Fe and Co investigated by ICP is close to 48:52. To study the effects of applying a 3 kOe magnetic field along the wire during the annealing process on the array's magnetic performance, the $Fe_{48}Co_{52}$ alloy nanowire arrays of Group M, which were annealed at temperatures ranging from 390 °C to 590 °C, were firstly selected for study. It was found that with the annealing temperature increasing, the coercivity H_c and the squareness M_r/M_s for all the annealed arrays had the same variation tendency. As an example, Figure 1 shows H_c and M_r/M_s of the array with D_w of about 22 nm and D_i of about 50 nm as a function of the annealing temperature. It should be noted here that H_c and M_r/M_s shown in this figure were measured with the applied magnetic field parallel to the wire axis. It is obvious that both H_c and M_r/M_s increase firstly and then decrease with the annealing temperature increasing. The enhancement of H_c with the annealing temperature increasing can be attributed to the increases of the saturation magnetization M_s and the crystallite size [21]. Because the arrays were annealed in the hydrogen atmosphere, the diffusion of Al into nanowire at high temperature, not the oxygenation of the nanowire [16,21], is believed to be the very reason for the deterioration of H_c with the annealing temperature increasing further. From Fig.1, we can also see that 550 °C is the best annealing temperature, at which both H_c and M_r/M_s reach their maximums. This is similar to the situation of annealing FeCo alloy nanowire arrays without applying a magnetic field [21].

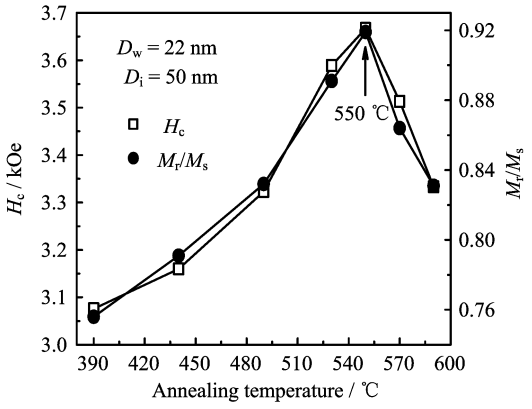

FIG. 1 Coercivity H_c and squareness M_r/M_s for $Fe_{48}Co_{52}$ alloy nanowire arrays (Group M) annealed at temperatures ranging from 390 °C to 590 °C. Both H_c and M_r/M_s were measured with the applied magnetic field along the wire.

DOI:10.1088/1674-0068/22/01/82-86
©2009 Chinese Physical Society

For the $Fe_{48}Co_{52}$ alloy nanowire arrays described in Fig.1, their XRD patterns were shown in Fig.2. It can be seen that all the arrays have a body-centred-cubic (bcc) structure and preferred (110) orientation along the axis of the wire. The patterns are similar to those of the $Fe_{48}Co_{52}$ alloy nanowire arrays annealed in hydrogen atmosphere without applying any magnetic field [23,24]. Here, we should note that this also holds true for all the other arrays discussed in this work. Obviously, applying a 3 kOe magnetic field during the annealing process and the variation of the annealing temperature does not have any apparent influence on the crystalline structure of the arrays. According to the previous reports, the array's crystalline structure mainly depends on its composition [13,19,20].

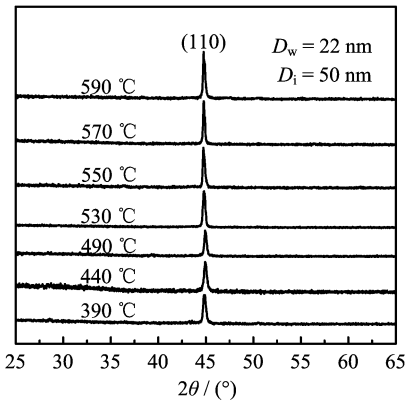

FIG. 2 XRD patterns of $Fe_{48}Co_{52}$ alloy nanowire arrays (Group M) annealed at temperatures ranging from 390 °C to 590 °C.

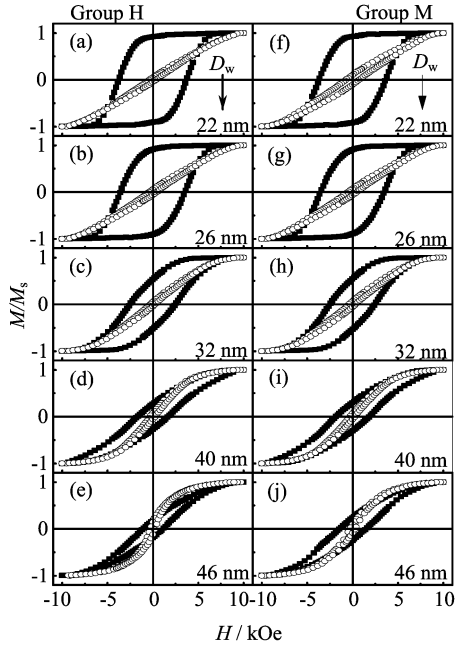

FIG. 3 Normalized hysteresis loops for the annealed arrays of (a)-(e) Group H and (f)-(j) Group M with the measuring magnetic field parallel (//, solid square) and perpendicular (⊥, hollow circle) respectively to the wire axis. The interwire distances D_i of the arrays are about 50 nm. All the arrays were annealed at 550 °C.

To study the influences of the magnetic field annealing on the arrays' magnetic performance, we also compared the magnetic properties for the annealed $Fe_{48}Co_{52}$ alloy nanowire arrays with different D_w and D_i of Group M with those of Group H. Here, the arrays annealed at 550 °C were selected as the studying objects. The normalized hysteresis loops of the annealed arrays with fixed D_i (50 nm) and various D_w (22-46 nm) and with fixed D_w (22 nm) and various D_i (30-60 nm) are shown in Fig.3 and Fig.4, respectively. It can be seen that for the arrays of both groups, with D_w increasing or D_i decreasing, the hysteresis loop measured with the applied magnetic field along the wire (parallel direction, //) becomes narrower and sheared, the easy magnetization direction gradually changes from the wire axis to the direction perpendicular to the wires (perpendicular direction, ⊥), and the saturation field H_s in the parallel direction increases while H_s in the perpendicular direction decreases. All these phenomena can be mainly attributed to the increase of the magnetostatic interaction between the wires with D_w increasing or D_i decreasing [23,24]. From these two figures, we can also see that applying a 3 kOe magnetic field along the wire during the annealing process constrains the easy magnetization direction shifting from the parallel direction to the perpendicular direction for the annealed arrays with D_w more than 40 nm or with D_i less than 40 nm.

To show the influence of the magnetic field annealing

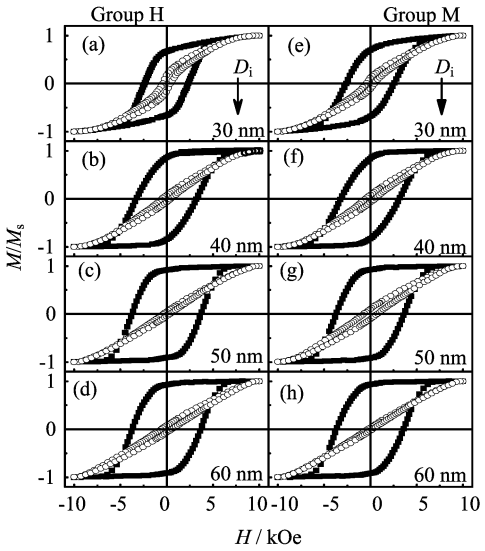

FIG. 4 Normalized hysteresis loops for the annealed arrays of (a)-(d) Group H and (e)-(h) Group M with the measuring magnetic field parallel (//, solid square) and perpendicular (⊥, hollow circle) respectively to the wire axis. The wire diameters D_w of the arrays are about 22 nm. All the arrays were annealed at 550 °C.

DOI:10.1088/1674-0068/22/01/82-86
©2009 Chinese Physical Society

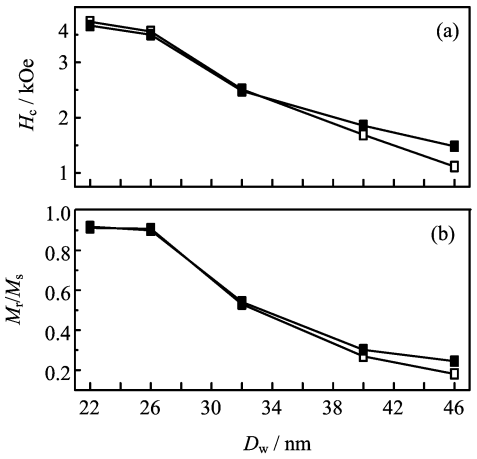

FIG. 5 (a) Coercivity H_c and (b) squareness M_r/M_s measured along the wire for the annealed arrays of Group H (hollow square) and Group M (solid square) as a function of the wire diameter D_w. The interwire distances D_i of the arrays are about 50 nm. All the arrays were annealed at 550 °C.

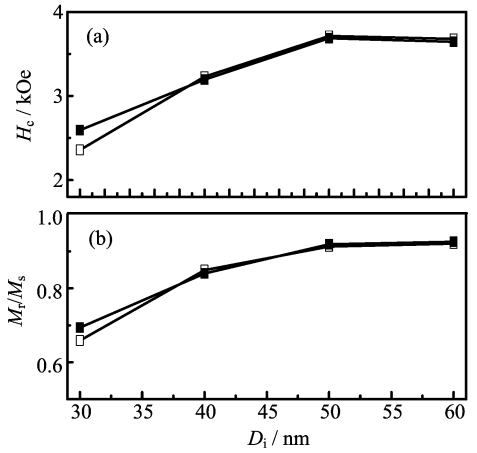

FIG. 6 (a) Coercivity H_c and (b) squareness M_r/M_s measured along the wire for the annealed arrays of Group H (hollow square) and Group M (solid square) as a function of the interwire distance D_i. The wire diameters D_w of the arrays are about 22 nm. All the arrays were annealed at 550 °C.

on the magnetic properties of $Fe_{48}Co_{52}$ alloy nanowire arrays more clearly, we exhibit the comparison of H_c and M_r/M_s measured along the wire for the annealed arrays of Group M and Group H in Fig.5 and Fig.6. Here, Figure 5 shows H_c and M_r/M_s of the arrays with fixed D_i (50 nm) and various D_w (22-46 nm), and Figure 6 shows those of the arrays with fixed D_w (22 nm) and various D_i (30-60 nm). It can be seen that for the arrays with D_w less than 32 nm or with D_i more than 40 nm, H_c and M_r/M_s of Group M are almost the same with those of Group H. However, H_c and M_r/M_s for the arrays with D_w more than 40 nm or with D_i less than 40 nm are improved obviously by applying a 3 kOe magnetic field along the wire during the annealing process and their growths increase with D_w increasing or D_i decreasing.

As reported previously, within a FeCo alloy nanowire array with large aspect ratio, the shape anisotropic field of the individual wires induces the magnetic moments parallel to the wire axis, while the magnetostatic interaction between the wires tends to reverse the magnetic moments [23,24]. The competition of the shape anisotropic field and the magnetostatic interaction field, usually simplified as an effective anisotropic field, is considered to be the main factor that determines the array's magnetization behavior in an external magnetic field [32,33]. Because applying a magnetic field along the wire during the annealing process also helps the magnetic moments align along the wire axis, it has a similar effect on the array's magnetic properties as the shape anisotropic field . Therefore, it can improve the magnetic performance of the array with a weak effective anisotropic field obviously. But for the array possessing a very strong effective anisotropic field, the effects caused by the magnetic field annealing are usually too tiny to be noticed. Based on these explanations, we can deduce that the arrays with D_w less than 32 nm or with D_i more than 40 nm possess a very strong shape anisotropic field and a relatively weak magnetostatic interaction field. As proved by the arrays' good hard magnetic properties (H_c>3.23 kOe, M_r/M_s>0.85), this results in a strong effective anisotropic field which induces most magnetic moments aligned along the wire. Therefore, applying a 3 kOe magnetic field along the wire could not enhance the magnetic properties of the annealed arrays noticeably. To further improve the magnetic performances of these arrays, increasing the magnetic field for annealing should be an effective way. For the arrays with D_w more than 40 nm or with D_i less than 40 nm, although the shape anisotropic fields of the individual wires are still very strong due to their large aspect ratios (L/D_w>43), the magnetostatic interaction between the wires keeps increasing with D_w increasing or D_i decreasing. Thus, the effective anisotropic field decreases gradually with the increase of D_w or the decrease of D_i. Correspondingly, the influence of the magnetic field annealing on the magnetic properties of these arrays shows up gradually and the enhancement of the magnetic performance becomes more and more remarkable.

IV. CONCLUSION

In conclusion, we studied the influence of magnetic field annealing on the properties of $Fe_{48}Co_{52}$ alloy nanowire arrays with different interwire distances (D_i=30-60 nm) and wire diameters (D_w=22-46 nm). It was found that applying a 3 kOe magnetic field along the wire during the annealing process had no apparent

DOI:10.1088/1674-0068/22/01/82-86 ©2009 Chinese Physical Society

effect on the best annealing temperature and the crystalline structure of the arrays, although it did affect the magnetic properties of these arrays differently. For the arrays with D_w less than 32 nm or with D_i more than 40 nm, applying a 3 kOe magnetic field along the wire during the annealing process had almost no influence on their magnetic performance. But for the arrays with D_w more than 40 nm or with D_i less than 40 nm, such a magnetic field annealing constrained the shift of the easy magnetization direction and improved H_c and M_r/M_s obviously. The difference in the intensity of the array's effective anisotropic field can be used to explain this different variation of the array's magnetic properties after magnetic field annealing.

V. ACKNOWLEDGMENTS

This work was supported by the National Nature Science Foundation of China (No.50171033), the National Key Project of Fundamental Research of China (No.2005CB623605), and the Scientific Research Foundation for the Doctor of Hefei University of Technology (No.035032).

[1] D. J. Sellmyer, M. Zheng, and R. Skomski, J. Phys.: Condens. Matter **13**, R433 (2001).
[2] R. Skomski, J. Phys.: Condens. Matter **15**, R841 (2003).
[3] M. Hernández-Vélez, Thin Solid Films **495**, 51 (2006).
[4] M. A. Kashi, A. Ramazani, and A. Khayyatian, J. Phys. D **39**, 4130 (2006).
[5] X. Y. Zhang, G. H. Wen, Y. F. Chan, R. K. Zheng, X. X. Zhang, and N. Wang, Appl. Phys. Lett. **83**, 3341 (2003).
[6] A. L. Friedman and L. Menon, J. Electrochem. Soc. **154**, E68 (2007).
[7] H. Zeng, M. Zheng, R. Skomski, D. J. Sellmyer, Y. Liu, L. Menon, and S. Bandyopadhyay, J. Appl. Phys. **87**, 4718 (2000).
[8] S. Kato, H. Kitazawa, and G. Kido, J. Magn. Magn. Mater. **272-276**, 1666 (2004).
[9] G. B, Ji, J. M. Cao, F. Zhang, G. Y. Xu, H. L. Su, S. L. Tang, B. X. Gu, and Y. W. Du, J. Phys. Chem. B **109**, 17100 (2005).
[10] G. C. Han, B. Y. Zong, and Y. H. Wu, IEEE Trans. Magn. **38**, 2562 (2002).
[11] T. R. Gao, L. F. Yin, C. S. Tian, M. Lu, H. Sang, and S. M. Zhou, J. Magn. Magn. Mater. **300**, 471 (2006).
[12] R. L. Wang, S. L. Tang, B. Nie, X. L. Fei, Y. G. Shi, and Y. W. Du, Solid State Commun. **142**, 639 (2007).
[13] Q. F. Zhan, Z. Y. Chen, D. S. Xue, F. S. Li, H. Kunkel, X. Z. Zhou, R. Roshk, and G. Williams, Phys. Rev. B **66**, 134436 (2002).
[14] G. Sharma, M. V. Pishko, and C. A. Grimes, J. Mater. Sci. **42**, 4738 (2007).
[15] J. P. Pierce, E. W. Plummer, and J. Shen, Appl. Phys. Lett. **81**, 1890 (2002).
[16] D. H. Qin, L. Cao, Q. Y. Sun, Y. Huang, and H. L. Li, Chem. Phys. Lett. **358**, 484 (2002).
[17] D. H. Qin, Y. Peng, L. Cao, and H. L. Li, Chem. Phys. Lett. **374**, 661 (2003).
[18] W. Chen, S. L. Tang, M. Lu, and Y. W. Du, J. Phys.: Condens. Matter **15**, 4623 (2003).
[19] P. S. Fodor, G. M. Tsoi, and L. E. Wenger, J. Appl. Phys. **93**, 7438 (2003).
[20] G. H. Lee, S. H. Huh, J. W. Jeong, S. H. Kim, B. J. Choi, H. C. Ri, B. Kim, and J. H. Park, J. Appl. Phys. **94**, 4179 (2003).
[21] S. L. Tang, W. Chen, M. Lu, S. G. Yang, F. M. Zhang, and Y. W. Du, Chem. Phys. Lett. **384**, 1 (2004).
[22] C. Jo, J. I. Lee, and Y. Jang, Chem. Mater. **17**, 2667 (2005).
[23] H. L. Su, G. B. Ji, S. L. Tang, W. Chen, Z. Li, B. X. Gu, and Y. W. Du, J. Appl. Phys. **97**, 116104 (2005).
[24] H. L. Su, G. B. Ji, S. L. Tang, Z. Li, B. X. Gu, and Y. W. Du, Nanotechnology **16**, 429 (2005).
[25] Z. K. Wang, H. S. Lim, V. L. Zhang, J. L. Goh, S. C. Ng, M. H. Kuok, H. L. Su, and S. L. Tang, Nano Lett. **6**, 1083 (2006).
[26] L. Cao, X. P. Qiu, J. B. Ding, H. L. Li, and L. Q. Chen, J. Mater. Sci. **41**, 2211 (2006).
[27] J. H. Gao, Q. F. Zhan, W. He, D. L. Sun, and Z. H. Cheng, J. Magn. Magn. Mater. **305**, 365 (2006).
[28] Y. W. Ma, K. Watanabe, S. Awaji, and M. Motokawa, Phys. Rev. B **65**, 174528 (2002).
[29] H. Y. Wang, X. K. Ma, Y. J. He, S. Mitani, and M. Motokawa, Appl. Phys. Lett. **85**, 2304 (2004).
[30] H. Masuda and K. Fukuda, Science **268**, 1466 (1995).
[31] Y. Li, G. W. Meng, L. D. Zhang, and F. Phillipp, Appl. Phys. Lett. **76**, 2011 (2000).
[32] M. Grimsditch, Y. Jaccard, and I. K. Schuller, Phys. Rev. B **58**, 11539 (1998).
[33] G. J. Strijkers, J. H. Dalderop, M. A. A. Broeksteeg, H. J. M. Swagten, and W. J. M. de Jonge, J. Appl. Phys. **86**, 5141 (1999).

DOI:10.1088/1674-0068/22/01/82-86 ©2009 Chinese Physical Society